Electronic Supplementary Information for

Cu(III)-bis-thiolato complex forms an unusual mono-thiolato Cu(III)-peroxido adduct

Jane M. Donnelly[a], Frederik Lermyte[b], Juliusz A. Wolny[c], Marc Walker[d], Ben Breeze[d], Russell J. Needham[e], Christina S. Müller[c], Peter B. O'Connor[e], Volker Schünemann[c], Joanna F. Collingwood[a], and Peter J. Sadler[e]*

[a]*School of Engineering, University of Warwick, Gibbet Hill Road, Coventry CV4 7Al, United Kingdom*

[b] *Department of Chemistry, Technical University of Darmstadt, Alarich-Weiss-Strasse 4, 64287 Darmstadt, Germany*

[c]*Department of Physics, Technische Universität Kaiserslautern , Erwin-Schrödinger-Straße 46, 67663 Kaiserslautern, Germany*

[d]*Department of Physics, University of Warwick, Gibbet Hill Road, Coventry CV4 7AL, United Kingdom*

[e] *Department of Chemistry, University of Warwick, Gibbet Hill Road, Coventry CV4 7AL, United Kingdom*

*Corresponding author email: P.J.Sadler@warwick.ac.uk

Table of Contents

1. Materials and Methods

Anhydrous copper(II) acetate ($Cu(OAc)_2$), toluene-3,4-dithiol, triethylamine, and methanol were all purchased from Sigma-Aldrich and used as received. Ultrahigh-resolution MS analysis was carried out on a 12 tesla Bruker solariX FTICR instrument. High resolution mass spectra were obtained using a Bruker maXis plus Q-TOF mass spectrometer equipped with electrospray ionisation source. The instruments were used in negative ion mode. NMR spectra were acquired in 5 mm NMR tubes at 25 ºC on a Bruker Avance III 400 MHz spectrometer. Data processing was carried out with Bruker TopSpin version 4.0.8. ^{1}H NMR chemical shifts were internally referenced to TMS *via* their residual solvent peaks (acetone $\delta = 2.05$ ppm). Spectra were recorded using standard pulse sequences. XPS spectra were obtained with a Kratos Axis Ultra DLD spectrometer. The EPR spectrum was obtained with a Bruker EMX X-Band 9.35 GHz spectrometer.

2. Synthesis and Characterization of [bis(toluene-3,4-dithiolato)copper(III)][NEt_3H] (NEt_3H·1)

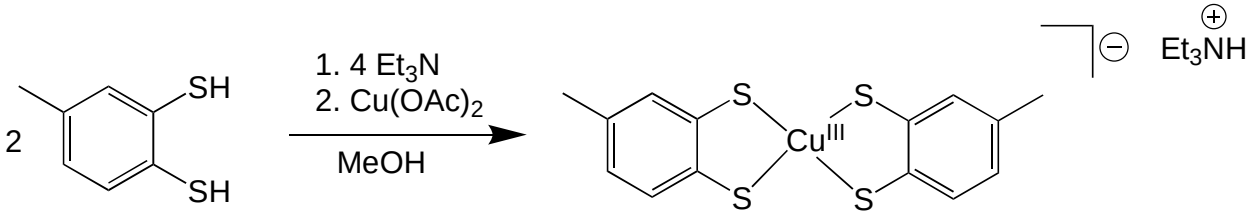

Triethylamine (Et_3N) (0.112 mL, 0.8 mmol, 4 mol eq) was added to a solution of toluene-3,4-dithiol (0.062 g, 0.4 mmol, 2 mol eq) in MeOH and stirred for 10 min. The mixture was then added dropwise to a solution of copper(II) acetate (0.036 g, 0.2 mmol, 1 mol eq) in MeOH and allowed to stir open to the air (source of O_2 as an electron acceptor) for 2 h. A dark green precipitate was collected by vacuum filtration and trace solvent was removed under reduced pressure. Yield: 0.059 g (61.7%). %). ^{1}H NMR (400 MHz, acetone-d_6): δ 6.78 (dd, aromatic, 4H), 6.73 (s, aromatic,

2H), 2.19 (s, aromatic-C*H*$_3$, 6H), 3.43 (q, NH-C*H*$_2$-CH$_3$, 6H), 1.42 (t, NH-CH$_2$-*CH*$_3$, 9H). UV-Vis (MeCN, 25°C): λ_{mzx} = 393 nm (ε = 7670 $M^{-1}cm^{-1}$), 323 nm (ε = 3680 $M^{-1}cm^{-1}$). ESI-MS calculated for $[C_{14}H_{12}S_4Cu]^-$: *m/z* 370.91233. Found: 370.91232. Calcd for $C_{20}H_{28}CuS_4N{\cdot}0.35\ H_2O$: C, 49.99; H, 6.02; N, 2.91. Found: C, 49.82; H, 5.34; N, 2.23.

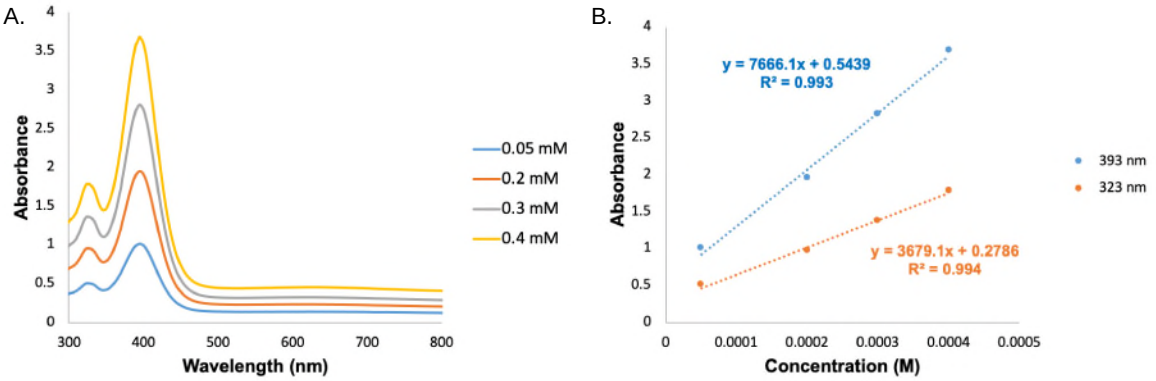

Figure S1. (A) UV-Vis spectra of [bis(toluene-3,4-dithiolato)copper(III)][NEt$_3$H] (NEt$_3$H·**1**) at concentrations of: 0.05 mM, 0.2 mM, 0.3 mM, and 0.4 mM in MeCN at 25°C. (B) Beer's Law plot for NEt$_3$H·**1.**

3. NMR

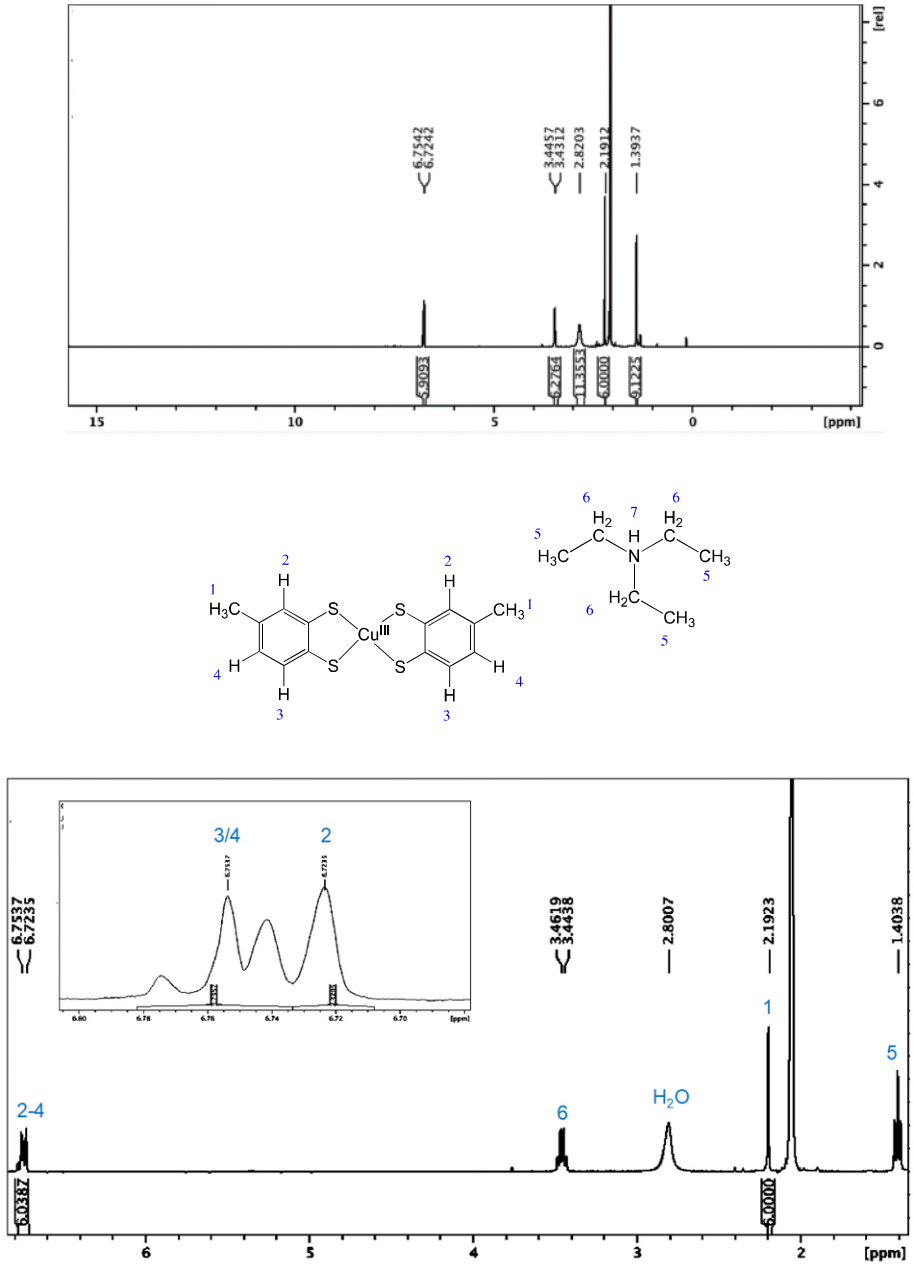

Figure S2. ^{1}H NMR spectrum of [bis(toluene-3,4-dithiolato)copper(III)][NEt_3H] (NEt_3H·**1**) in acetone-d_6 at 25°C. Above: -5 to 15 ppm. Below: peaks showing assignments. Slight broadening of peaks is attributable to the presence of a trace of paramagnetic Cu(II). The NH peak is likely to be broadened by exchange with H_2O.

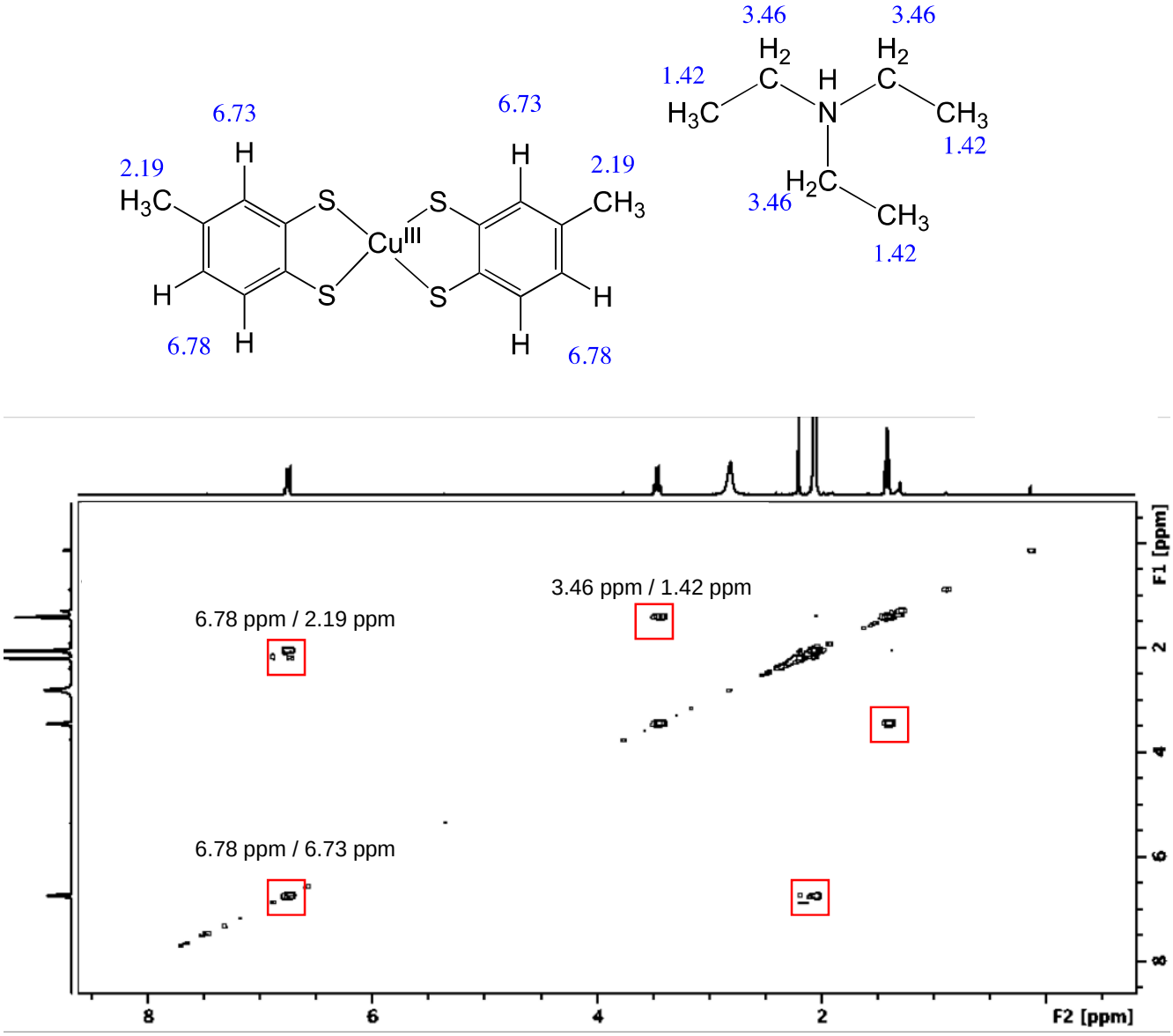

Figure S3. COSY spectrum of [bis(toluene-3,4-dithiolato)copper(III)][NEt_3H] (NEt_3H·**1**) in acetone-d_6 at 25°C showing cross peaks consistent with the structure of complex **1**. For expansion of aromatic region see Fig. S4.

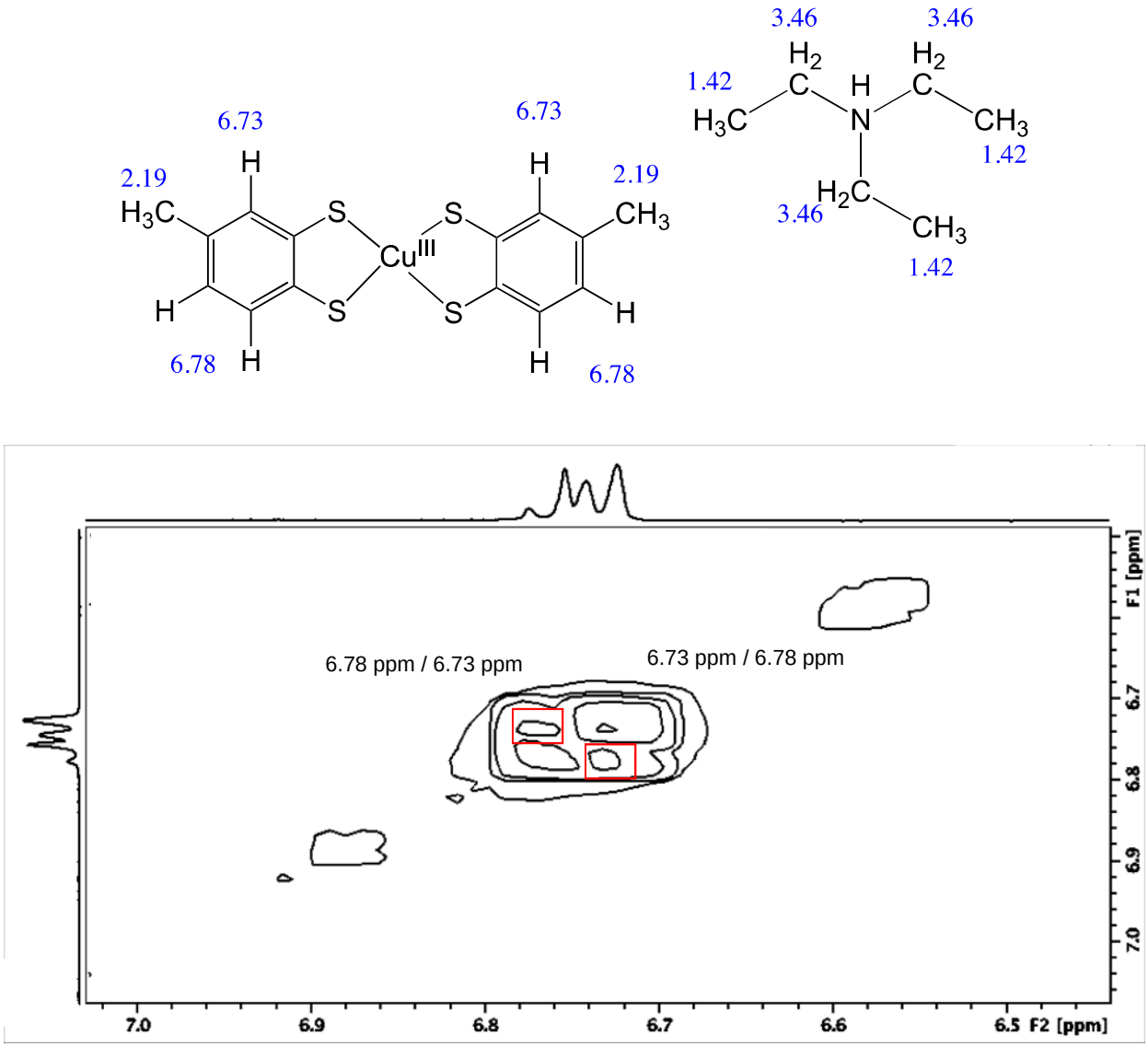

Figure S4. Aromatic region of the COSY spectrum of [bis(toluene-3,4-dithiolato)copper(III)][NEt_3H] (NEt_3H·**1**) in acetone-d_6 at 25°C.

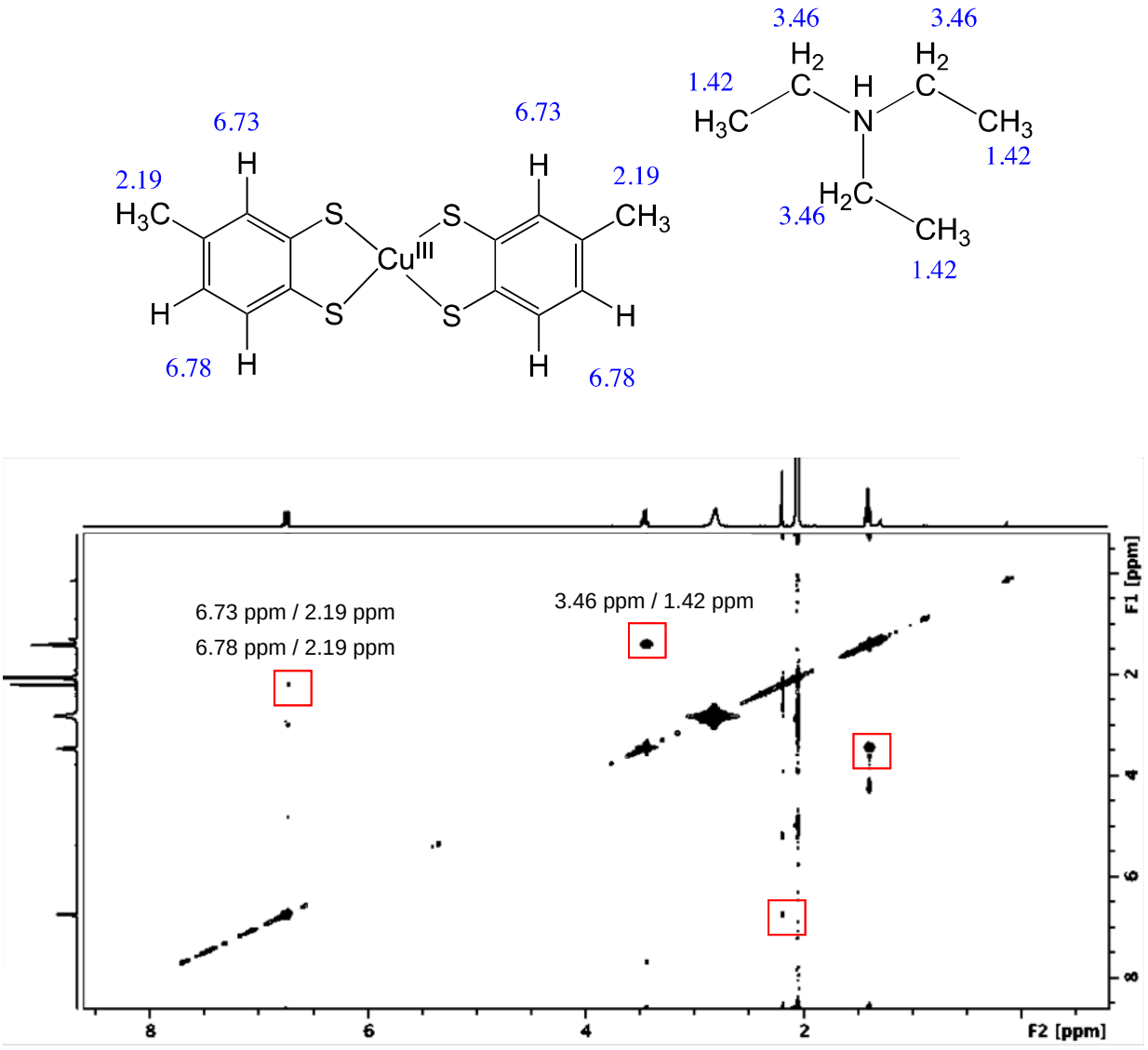

Figure S5. NOESY spectrum of [bis(toluene-3,4-dithiolato)copper(III)][NEt_3H] (NEt_3H·**1**) in acetone-d_6 at 25°C.

4. Mass Spectrometry

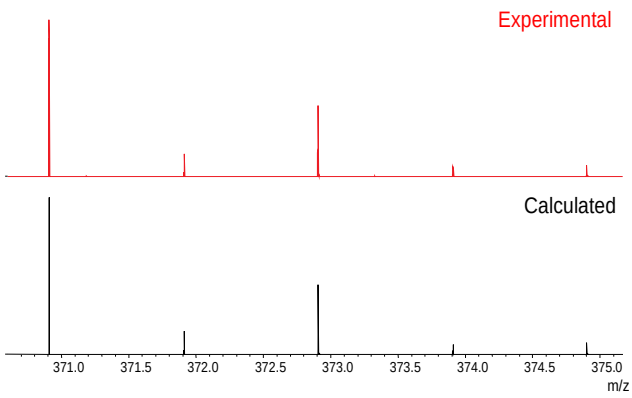

Figure S6. Experimental and calculated UHR-MS spectrum of **1**.

Table S1. Calculated and observed negative ion mode MS peaks for [bis(toluene-1,2-dithiolato)copper(III)]$^-$ (**1**) (where A is the highest intensity peak relative to those listed in the table).

Peak	Observed (Da)	Calculated (Da)	Mass error (ppm)[a]
A	370.91232	370.91233	-0.027
A+1	371.91572	371.91569	0.081
A+2	372.91053	372.91052	0.027
A+3	373.91392	373.91388	0.107
A+4	374.90635	374.90632	0.080

[a] The mass errors in Tables S1-S3 are below 0.11 ppm, about 0.03 mDa at this mass, or less than 10% of the mass of an electron.

Table S2. Calculated and observed negative ion mode MS peaks for [(toluene-1,2-dithiolato)copper(I)]$^-$ (**2**) (where A is the highest intensity peak relative to those listed in the table).

Peak	Observed (Da)	Calculated (Da)	Mass error (ppm)
A	216.92123	216.92124	-0.046
A+1	217.9246	217.92459	0.046
A+2	218.91944	218.91943	0.046
A+3	219.9228	219.92279	0.045
A+4	220.91523	220.91523	0.000

Table S3. Calculated and observed negative ion mode MS peaks for [bis(toluene-1,2-dithiolato)copper(III)-peroxide]$^-$ (**3**) (where A is the highest intensity peak relative to those listed in the table).

Peak	Observed (Da)	Calculated (Da)	Mass error (ppm)
A	248.91107	248.91109	-0.064
A+1	249.91442	249.91443	-0.040
A+2	250.90924	250.90926	-0.080
A+3	251.91262	251.91262	0.000
A+4	252.90506	252.90506	0.000

Table S4. Calculated and observed negative ion mode isotopic fine structure for [bis(toluene-1,2-dithiolato)copper(III)-peroxide]$^-$ (**3**) (where A is the highest intensity peak relative to those listed in the table).

Formula[a]	Observed (Da)	Calculated (Da)	Mass error (ppm)	Intensity relative to most abundant (%)	Calculated intensity relative to most abundant (%)
A+1					
$^{63}Cu^{32}S_2{}^{1}H_6{}^{12}C_6{}^{13}C{}^{16}O_2$	249.91442	249.91442	0.000	7.04	7.57
$^{63}Cu^{32}S^{33}S{}^{1}H_6{}^{12}C_7{}^{16}O_2$	249.91046	249.91046	0.000	1.25	1.58
A+2					
$^{65}Cu^{32}S_2{}^{1}H_6{}^{12}C_7{}^{16}O_2$	250.90924	250.90926	-0.080	44.91	44.56
$^{63}Cu^{32}S^{34}S{}^{1}H_6{}^{12}C_7{}^{16}O_2$	250.90687	250.9069	-0.120	7.92	8.95
$^{63}Cu^{32}S_2{}^{1}H_6{}^{12}C_7{}^{16}O^{18}O$	250.91535	250.91531	0.159	0.46	0.41
A+3					
$^{65}Cu^{32}S_2{}^{1}H_6{}^{12}C_6{}^{13}C{}^{16}O_2$	251.91262	251.91261	0.040	3.06	3.37
$^{63}Cu^{32}S^{34}S{}^{1}H_6{}^{12}C_6{}^{13}C{}^{16}O_2$	251.91023	251.91022	0.040	0.58	0.7
$^{65}Cu^{32}S^{33}S{}^{1}H_6{}^{12}C_7{}^{16}O_2$	251.90867	251.90865	0.079	0.62	0.68
A+4					
$^{65}Cu^{32}S^{34}S{}^{1}H_6{}^{12}C_7{}^{16}O_2$	252.90506	252.90506	0.000	3.07	3
$^{65}Cu^{32}S_2{}^{1}H_6{}^{12}C_7{}^{16}O^{18}O$	252.91349	252.91351	-0.079	0.23	0.21
$^{65}Cu^{32}S_2{}^{1}H_6{}^{12}C_5{}^{13}C_2{}^{16}O_2$	252.91605	252.91597	0.316	0.09	0.11

In this Table the isotopic fine structure for peroxido adduct **3**, from A+1 up to A+4, is assigned with both the *m/z* and intensity of the fine structure peaks matching well.

Given the characteristic isotope abundances and mass defects for Cu and S, the formula assignment for the peroxido adduct is definitive. Effectively the number of C, O, S, and Cu atoms in the complex can be counted.

5. Cyclic Voltammetry

Cyclic voltammetry was performed on a solution of NEt_3H·**1** (1 mM) in acetonitrile (5 mL), with *n*-tetrabutylammonium hexafluorophosphate (0.1 M) as a supporting electrolyte. A polished platinum working electrode, platinum wire auxiliary electrode, and $Ag/AgNO_3$ reference electrode (0.1 M $AgNO_3$ in acetonitrile) were used. The electrolyte and complex mixture was purged with N_2 for 5 min prior to analysis. The analyte was scanned at a rate of 100 mV/s between 0.5 to -1.5 V. All measurements are reported vs. the Fc^+/Fc redox couple which is +640 mV vs. NHE.

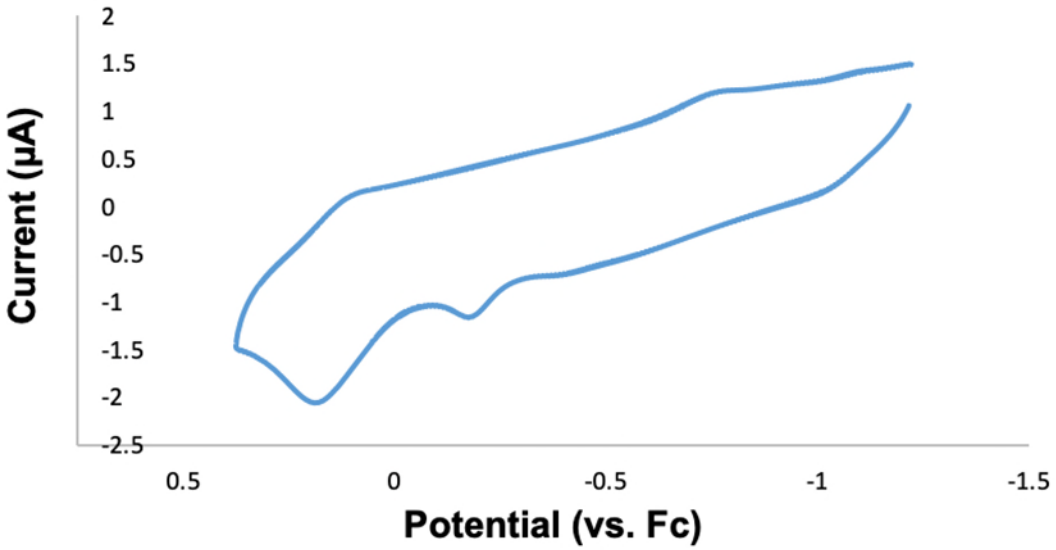

Figure S7. Cyclic voltammogram of [bis(toluene-3,4-dithiolato)copper(III)][NEt_3H] **(**NEt_3H·**1**) (1mM, MeCN) in the presence of *n*-tetrabutylammonium hexafluorophosphate (0.1 M). $E_{red,1}$ = -187 mV; $E_{ox,1}$ = -781 mV; ΔE_1 = 594 mV. $E_{red,2}$ = 181 mV; $E_{ox,2}$ = 83 mV. ΔE_2 = 98 mV.

6. Electron Paramagnetic Resonance

The EPR spectrum was recorded on a Bruker EMX X-Band 9.35 GHz spectrometer (equipped with a Bruker ER 4122 HS cylindrical resonator). All data were collected using a modulation amplitude a 0.1 mT and 100 kHz with an acquisition time of 40.96 ms at non saturating microwave powers and is the presented data is the average of 10 accumulations. Cavity and spectrometer background have been subtracted from the data. Quantitative estimation was achieved by comparison to a diamond containing 1.35 x 10^{19} spins/g ppm Ns0, a well characterised reference sample. In the absence of a simulation, the entire spectrum was integrated, so the reported concentration of the paramagnetic species (1.39 x 10^{20} spins/g) is an upper limit, including all background and radical spins.

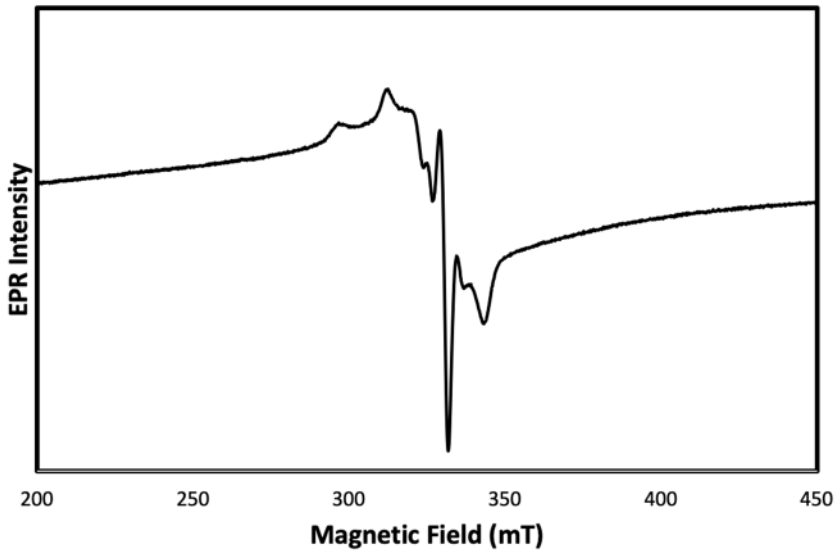

Figure S8. X-band electron paramagnetic resonance (EPR) spectrum for the product mixture of the synthesis for [bis(toluene-3,4-dithiolato)copper(III)][NEt_3H] **(**NEt_3H·**1)** (powder at 298 K).

7. X-ray Photoelectron Spectroscopy

The X-ray photoelectron spectroscopy (XPS) data were collected at the Warwick Photoemission Facility, University of Warwick. The samples investigated in this study were attached to electrically-conductive carbon tape, mounted on to a sample bar and loaded in to a Kratos Axis Ultra DLD spectrometer which possesses a base pressure around 2 x 10^{-10} mbar.

XPS measurements were performed in the main analysis chamber, with the sample being illuminated using a monochromated Al Kα X-ray source (hν = 1486.7 eV). The measurements were conducted at room temperature and at a take-off angle of 90° with respect to the surface parallel. The core level spectra were recorded using a pass energy of 20 eV (resolution approx. 0.4 eV), from an analysis area of 300 μm x 700 μm. The work function and binding energy scale of the spectrometer were calibrated using the Fermi edge and $3d_{5/2}$ peak recorded from a polycrystalline Ag sample prior to the commencement of the experiments. In order to prevent surface charging the surface was flooded with a beam of low energy electrons throughout the experiment and this necessitated recalibration of the binding energy scale during data analysis. To achieve this, the main C-C/C-H component of the C 1*s* spectrum was referenced to 285.0 eV. The data were analysed in the CasaXPS package, using Shirley backgrounds and mixed Gaussian-Lorentzian (Voigt) and modified Lorentzian lineshapes, with asymmetry included for any sp^2 carbon detected. For compositional analysis, the analyser transmission function has been determined using clean metallic foils to determine the detection efficiency across the full binding energy range.

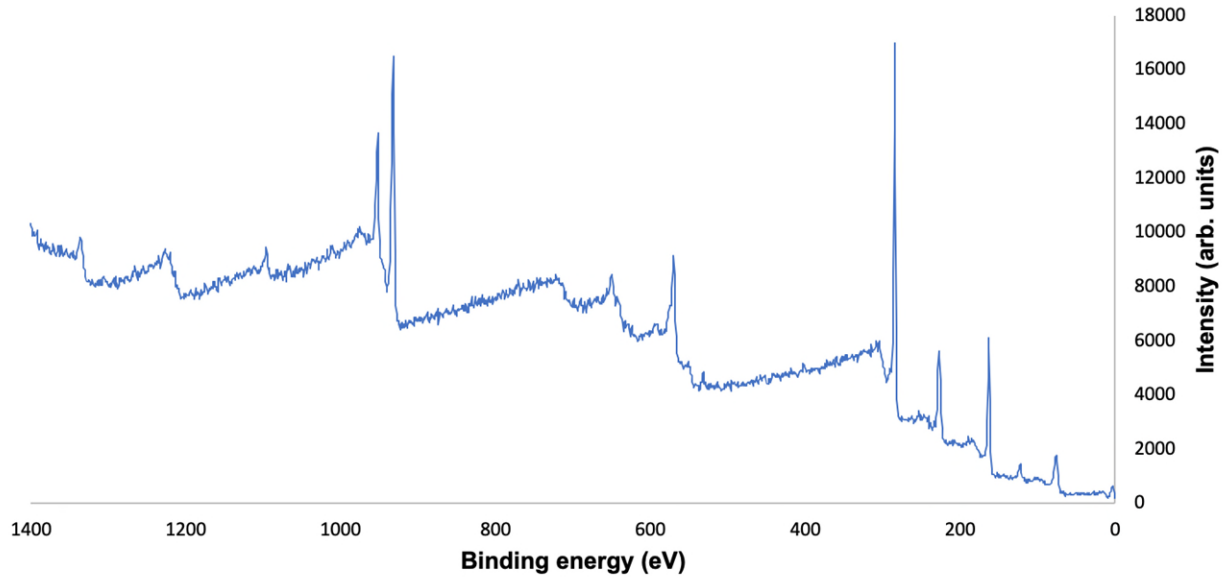

Figure S9. Full x-ray photoelectron spectrum of [bis(toluene-3,4-dithiolato)copper(III)][NEt_3H] (NEt_3H·**1**).

8. Density Functional Theory Calculations

The optimisation and UV-Vis calculations were performed with Gaussian 19[1] package, using the TPSS[2] density functional and qzvp[3] basis set. UV-Vis spectra were calculated with use of the TD (time dependent DFT) option of Gaussian with modeling of the solvent by the Polarizable Continuum Model (PCM) using the integral equation formalism variant (IEFPCM) for acetonitrile was applied for the TD DFT calculations. The broken symmetry[4] calculations were performed using the ORCA[5] package with a TPSS functional and tzvp[1] basis set and D3 dispersion correction.[6]

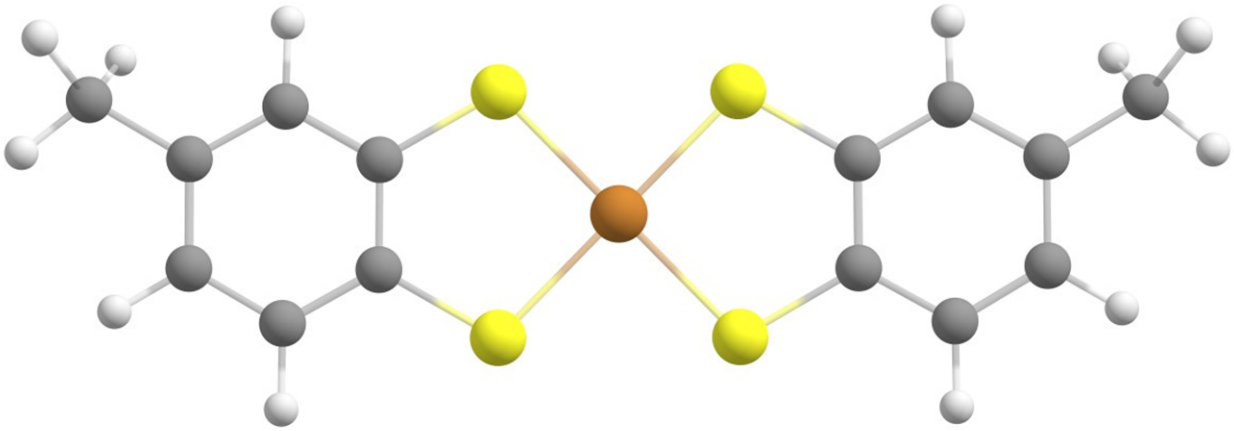

Figure S10. Optimized geometry of the bis(toluene-3,4-dithiolato)copper(III) anion (**1**).

Table S5. Calculated electrostatic potential-derived (ESP) charges of bis(toluene-3,4-dithiolato)copper(III) (**1**).[7]

Atom	ESP charge
Cu	0.497315
S	-0.374054
S	-0.380914
S	-0.374051
S	-0.380956

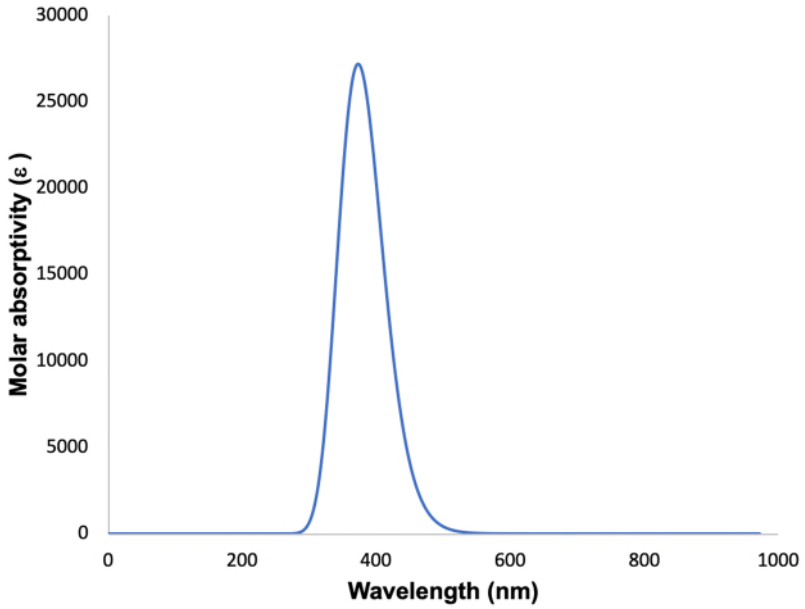

Figure S11. Calculated molar absorptivity for NEt_3H·**1**; λ_{max} = 374 nm (ε = 27000 $M^{-1}cm^{-1}$).

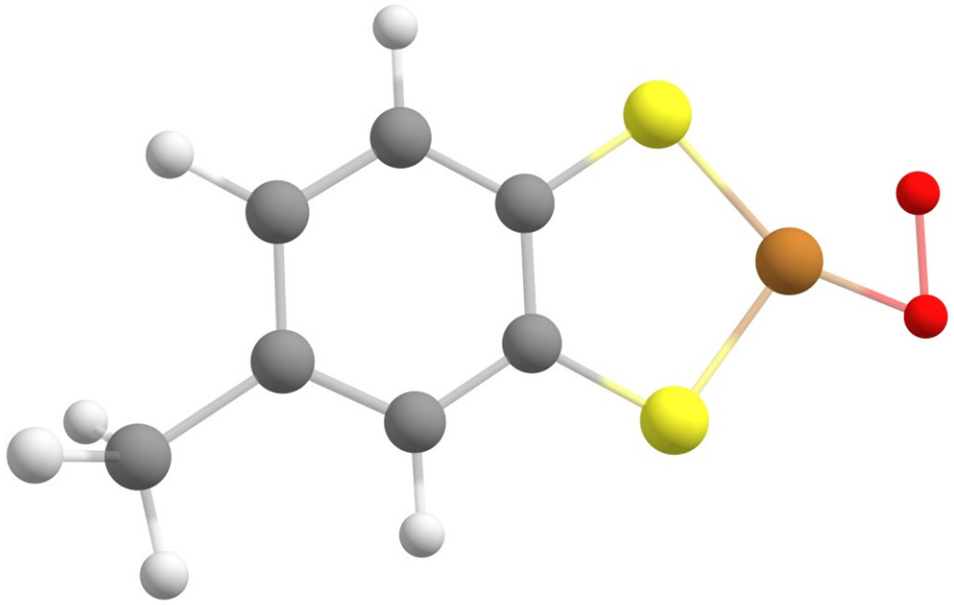

Figure S12. Optimized geometry of the (toluene-3,4-dithiolato)copper(III) peroxide anion (**3**).

Table S6. O-O bond distances for representative O_2-containing compounds, where L^2CuO_2 = ((2-(1-(2,6-di-isopropylphenylimino)ethyl)phenyl)(2,6-di-isopropylphenyl)amido-*N*,*N*′)-peroxo-copper(III) and L^1CuO_2 = *N*,*N*′-bis(2,6-diisopropylphenyl)-2,2,6,6-tetramethyl-3,5-heptanediiminato)-(peroxo-*O*,*O*′)-copper(III).[8-11]

Compound	O-O Bond Length (Å)
3	1.408
O_2^{2-} [for BaO_2]	1.49
O_2^- [for KO_2]	1.28
L^2CuO_2	1.392(3)
L^1CuO_2	1.392(12)

Table S7. Calculated Mulliken charges with hydrogens summed into heavy atoms for the singlet state of the (toluene-3,4-dithiolato)copper(III) peroxide anion (**3**).

Atom	Mulliken charge
Cu	0.777196
O	-0.356561
O	-0.357568
S	-0.494566
S	-0.496764

Table S8. Mulliken charges calculated for three Cu-O_2 compounds. Where L^2CuO_2 = ((2-(1-(2,6-di-isopropylphenylimino)ethyl)phenyl) (2,6-di-isopropylphenyl)amido-N,N')-peroxo-copper(III) and L^1CuO_2 = N,N'-bis(2,6-diisopropylphenyl)-2,2,6,6-tetramethyl-3,5-heptanediiminato)-(peroxo-O,O')-copper(III).[10-11]

Compound	Cu	O1	O2	L
3	0.777	-0.357	-0.358	-1.06
L^2CuO_2	0.70	-0.27	-0.27	-0.26
L^1CuO_2	0.68	-0.30	-0.30	-0.08

Table S9. Calculated electrostatic potential-derived (ESP) charges f or the singlet state of the (toluene-3,4-dithiolato)copper(III) peroxide anion (**3**).[7]

Atom	ESP charge
Cu	0.605464
O	-0.316903
O	-0.318144
S	-0.489694
S	-0.489918

References

1. Gaussian 16, Revision A.03,

   M. J. Frisch, G. W. Trucks, H. B. Schlegel, G. E. Scuseria, M. A. Robb, J. R. Cheeseman, G. Scalmani, V. Barone, G. A. Petersson, H. Nakatsuji, X. Li, M. Caricato, A. V. Marenich, J. Bloino, B. G. Janesko, R. Gomperts, B. Mennucci, H. P. Hratchian, J. V. Ortiz, A. F. Izmaylov, J. L. Sonnenberg, D. Williams-Young, F. Ding, F. Lipparini, F. Egidi, J. Goings, B. Peng, A. Petrone, T. Henderson, D. Ranasinghe, V. G. Zakrzewski, J. Gao, N. Rega, G. Zheng, W. Liang, M. Hada, M. Ehara, K. Toyota, R. Fukuda, J. Hasegawa, M. Ishida, T. Nakajima, Y. Honda, O. Kitao, H. Nakai, T. Vreven, K. Throssell, J. A. Montgomery, Jr., J. E. Peralta, F. Ogliaro, M. J. Bearpark, J. J. Heyd, E. N. Brothers, K. N. Kudin, V. N. Staroverov, T. A. Keith, R. Kobayashi, J. Normand, K. Raghavachari, A. P. Rendell, J. C. Burant, S. S. Iyengar, J. Tomasi, M. Cossi, J. M. Millam, M. Klene, C. Adamo, R. Cammi, J. W. Ochterski, R. L. Martin, K. Morokuma, O. Farkas, B. Foresman, and D. J. Fox, Gaussian, Inc., Wallingford CT, 2016.

2. J. M. Tao, J. P. Perdew, V. N. Staroverov and G. E. Scuseria, *Phys. Rev. Lett.*, 2003, **91** 146401.
3. a) A. Schäfer, C. Huber and R. Ahlrichs, *J. Chem. Phys.* 1994, **100**, 5829-5835. b) A. Schäfer, H. Horn, R. Ahlrichs, *J. Chem. Phys.* 1992, **97**, 2571-2577.
4. L. Noodleman, *J. Chem. Phys.* 1981**, 74**, 5737-5743.
5. F. Neese, *WIREs Comput. Mol. Sci.*, 2012, **2**, 73-78.
6. S. Grimme, J. Antony, S. Ehrlich, and H. Krieg, *J. Chem. Phys.*, 2010, **132**, 154104-19.
7. C. M. Breneman and K. B. Wiberg, *J. Comp. Chem.*, 1990, **11**, 361-373.
8. W. Wong-Ng and R. S. Roth, *Phys. C: Superconduc.*, 1994, **233**, 97-101.

9. S. C. Abrahams and J. Kalnajs, *Act. Cryst.*, 1955, **8**, 503-506.
10. N. W. Aboelella, S. V. Kryatov, B. F. Gherman, W. W. Brennessel, V. G. Young, Jr., R. Sarangi, E. V. Rybak-Akimova, K. O. Hodgson, B. Hedman, E. I. Solomon, C. J. Cramer and W. B. Tolman, *J. Am. Chem. Soc.*, 2004, **126**, 16896-16911.
11. A. M. Reynolds, B. F. Gherman, C. J. Cramer and W. B. Tolman, *Inorg. Chem.*, 2005, **44**, 6989-6997.